

Material Properties of High-Strength High Chromium TWIP Steel with Increased Corrosion Resistance

Pavel Podaný (0000-0002-1598-6058)¹, Tomáš Studecký (0000-0001-9611-7809)¹, Aleksandra Kocijan (0000-0002-2207-2254)²

¹COMTES FHT a.s., Průmyslová 995, 334 41, Dobřany, Czech Republic, E-mail: pavbel.podany@comtesfht.cz

²IMT - Institute of Metals and Technology, Lepi pot 11, 1000 Ljubljana, Slovenia. E-mail: Aleksandra.Kocijan@imt.si

Twinning induced plasticity (TWIP) steels are a class of high-strength steels that have been developed for their outstanding ductility and strength properties. TWIP refers to the fact that these steels display an unusually high degree of deformation before fracture due to the formation of twins during deformation. TWIP steels could be used in a variety of industries for structural applications or components that need to withstand high levels of stress and deformation. This article deals with the development of high strength with fully austenitic microstructure and high chromium content. Microstructure, mechanical and corrosion properties of this steel were studied.

Keywords: TWIP, Steels, Microstructure, Mechanical properties, Corrosion

1 Introduction

Steel is still the most widely used material for the production of car bodies and the continuous advances in the automotive industry have created a demand for strong and ductile steels that must exhibit high strength along with high ductility [1]. For components subjected to front- and rear-end impacts, high energy absorption is required if occupant injury is to be avoided. In side impact or in the event of a rollover onto the roof, intrusion protection is again required [2]. High manganese TWIP (Twinning Induced Plasticity) steels, which are highly ductile and high strength, are particularly suitable for deformation zones in the manufacture of components. They are austenitic steels characterized by a high degree of strengthening due to the twinning mechanism, which retain the ability of high deformation [3], [4]. TWIP steels derive their exceptional properties from a specific strengthening mechanism called twinning. The formation of mechanical twins during deformation produces high strain hardening, preventing necking and thus maintaining a very high load capacity. The high increase in the strengthening coefficient is due to the formation of a finer grained microstructure by the fact that the boundaries of the twins formed behave similarly to the grain boundaries and a strengthening of the steel occurs [5].

The main alloying element in TWIP steels is manganese (Mn). It is the high manganese content (15-33%) that ensures the formation of austenitic microstructure. In addition, these steels are alloyed with other elements such as silicon (Si), aluminium (Al), chromium (Cr) or nitrogen (N) to improve the desired

properties [3]. Small amounts of Mn have a pronounced hardening effect due to the formation of α' -martensite. Higher concentrations of Mn lead to the formation of ϵ -martensite. Both types of martensite are also formed by transformation of austenite under induced stress or strain. In the Fe-Mn binary system, a minimum of 27 % wt. Mn is required to obtain a stable austenite phase. At lower Mn contents, the formation of α' -martensite and ϵ -martensite needs to be suppressed by the addition of carbon. A carbon addition of about 0.6 % wt.% allows a homogeneous austenitic structure without carbide to be obtained, while the formation of ϵ -martensite is suppressed. The presence of hexagonal epsilon martensite is then often associated with the susceptibility of the steel to cracking due to hydride. Higher amounts of carbon can lead to carbide formation [6].

Alloying with Cr decreases the stacking fault energy (SFE) of Cr-alloyed steel and thus promotes twinning deformation at the expense of slip deformation [3, 7]. Chromium also increases the solubility of nitrogen (with a similar effect on SFE) both in the liquid state and in austenite [8, 9]. When alloying with chromium up to 15 wt.%, chromium has a positive effect on the yield strength [10] and also on ductility [11]. In general, chromium alloying has a positive effect on the formation of a passivation surface layer and thus an increase in corrosion resistance [11-13]. However, higher amounts of chromium can then lead to the precipitation of carbides during heat treatment, which have a negative effect on both corrosion resistance and toughness [11]. Carbides can be dissolved with the help of solution treatment, but this in turn can have a

negative effect on grain size.[13]. Yuan et al. also observed that as the Cr content of the matrix increases, the grain size decreases [14].

There are very few research papers dealing with the topic of corrosion in TWIP steels. The corrosion resistance of standard TWIP steels is not good and there is an attempt to improve this property by alloying other elements such as chromium and aluminium, which should provide passivation and corrosion resistance. Few studies have been carried out on the alloying of TWIP steels with chromium from 2 to 12 wt. % mostly in combination with aluminium alloying [15-17]. Mujica et al combined 11.89 wt. % of Cr with 21.09 Mn and no Mo [18]. The alloying concept chosen in the experiment of this paper was focused on alloying with high manganese (ca 28 wt. %) and increased Cr (above 12.5 wt. %), Mo content of ca 1.3 wt. % and N content of ca 0.7 wt. % for increasing of corrosion resistance. No aluminium was alloyed in steel in this study. In addition to increased corrosion resistance, the aim was to achieve an ideal combination of high strength and high ductility of over 50%.

2 Materials and methods

The experimental steel was melted and cast in a vacuum induction furnace into an ingot with a round cross-section. The chemical composition (see Table 1) was measured on the sample by means of optical emission spectrometer BRUKER Q8 Magellan. After cooling, the ingot was heated in the furnace to a rolling temperature of 1100 °C. The ingot was then hot rolled

on an experimental rolling mill to a sheet thickness of 9 mm. The surface of the sheet was then descaled by sandblasting and further cold rolled to a sheet thickness of 4 mm. After cold rolling, annealing was carried out in a vacuum furnace at 950 °C for 2 hours. The main objective of this annealing was to recrystallize the microstructure to ensure an increase in the plasticity of the experimental steel. The phase composition was measured using X-ray diffraction on the cold rolled and recrystallized annealed sheet samples. The microstructure of the steel was documented using a JEOL IT 500 HR scanning electron microscope and a EBSD camera Hikari super by EDAX. Tensile tests were carried out according to EN ISO 6892-1 (Metallic materials – Tensile testing – Part 1: Test method at room temperature) on a Zwick/Roell 250 kN 110 electromechanical testing machine. The deformation was measured using a strain gauge extensometer. An experimental steel specimen with a grinded surface was used to measure the corrosion properties. Gamry PC4 electrochemical potentiostat was used for corrosion tests. The test was carried out at 21°C in model seawater containing 3.5 wt.% NaCl. The samples were stabilised at the open circuit potential (E_{oc}) for 3600 s. The polarisation resistance (R_p) was measured within ± 0.02 V/ E_{oc} at a scan rate of 0.125 mV/s. The cyclic polarisation curve was measured in the range of -0.2 V/ E_{oc} to 1.2 V/ E_{oc} at a scan rate of 0.5 mV/s. A pressure cell was used for the measurements. A Pt counter electrode and a silver chloride reference electrode (ACLE) were used for all measurements.

Tab. 1 Chemical composition of experimental steel

Element	C	Mn	Cr	Si	Mo	N	Cu	P	S	Fe
[wt. %]	0.38	27.80	12.70	0.15	1.26	0.73	0.034	0.018	0.001	bal.

3 Results and discussion

3.1 Mechanical properties

The tensile test was carried out on three specimens of sheet metal after recrystallization annealing. Three samples (B1 - B3) were tested. The test results (yield strength - YS, tensile strength - TS, elongation - El and reduction of area - RA) are summarised in Table 2. Figure 1 shows the engineering stress-strain curves. All samples showed a good combination of high strength and ductility. Good ductility is also a result of the 0.73 nitrogen alloying, which is consistent with research by Yung et al. [9] where they proved that N is very effective in improving the mechanical properties. As will be demonstrated below, the high ductility is also the result of the plasticity of the material due to the intense twinning of austenitic grains induced by deformation. Comparing the mechanical properties of this experimental steel with

dual-phase steels (e.g. DP800 in [19]), which are nowadays commonly used for car body parts in the automotive industry for their good combination of strength and ductility [20, 21], it is evident that in the values of ultimate tensile strength the experimental steel is comparable to DP800 (846 MPa in [19] contra 941 MPa here) and in the value of ductility it is more than three times higher (16.92 % in [19] contra 54.5 % here). This means that when using a component from this experimental steel for the deformation zones, the component absorbs multiple values of impact energy. Experimental steel also shows better YS and TS in comparison to the research of Mujica et al in [18] with TWIP steel with similar chromium content (11.89 wt. %). They obtained YS - 430 MPa and TS – 840 MPa. Compared to the research on 24Mn6.3Cr0.2N steel in the study of Wang et al [22], better yield strength and ultimate strength values (YS = 423 MPa and TS 906 MPa in [22] but lower ductility (70% in [20]) were

achieved. The lower ductility of the experimental steel from this research compared to [22] can be attributed to the higher hardening due to the alloying with higher chromium content.

Tab. 2 Mechanical properties of experimental steel

YS [MPa]	TS [MPa]	El [%]	RA [%]
517.3 ± 4.4	941.5 ± 2.5	54.5 ± 2.0	43.7 ± 3.9

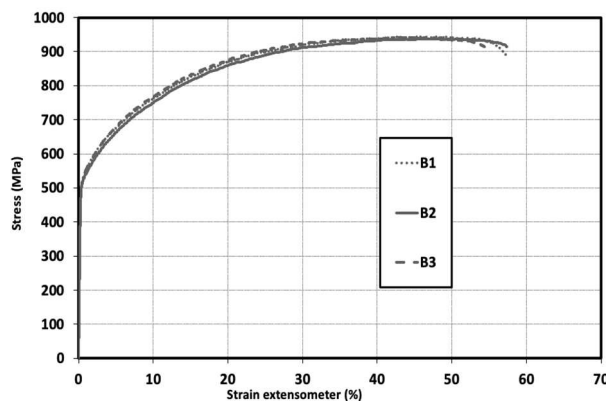


Fig. 1 Engineering stress-strain curves of experimental steel

3.2 Microstructural properties

X-Ray diffraction of the samples in the cold-rolled and recrystallization annealed states shows the presence of only the austenitic phase. Thus, it is shown that only twinning of austenitic grains occurs in the microstructure during intense plastic deformation. It is thus shown by diffraction (see Fig. 2) that there is no strain-induced transformation of austenite to either alpha' martensite or epsilon martensite (i.e. martensite with HCP lattice) in this experimental steel. The absence of this phase is important for prevention of delayed hydrogen cracking which was studied by Chun et al [6]. They observed, that that the gamma/epsilon interfaces are mainly responsible for severe hydrogen embrittlement where hydrogen cause decreasing of the bonding force at the interface and this effect has a negative influence on mechanical properties. Nevertheless, this phenomenon should not be present in this experimental steel because, as mentioned above, epsilon martensite was not observed in both the annealed state and in the state after intense plastic deformation during cold rolling.

Several etching reagents (including various tint etchants) have been tried to etch the microstructure for documentation purposes, but none have been successful in making the grains visible without unwanted artifacts unrelated to the structural components. In the end, the technique of documenting the as-polished microstructure in a row electron microscope, at low electron beam

accelerating voltage (5 kV), low viewing distance (6 mm) and in the back-reflected electron (BSE) mode proved to be the most useful. Figure 3 thus shows the microstructure of austenitic grains with twins that are clearly visible due to the sensitive BSE detector.

EBSD analysis of the microstructure performed on annealed microstructure is shown in Fig. 4(a). High-angle grain boundaries (15 - 65°) are highlighted by the black line, the boundaries between twins by the red line. The grain size analysis (see Figure 4 b) was performed in OIM Analysis software (EDAX) according to ASTM E 112 (Standard Test Methods for Determining Average Grain Size). The result of the analysis showed that the average grain size obtained after recrystallization annealing is $G = 12.6$, which can be considered as a very fine grained microstructure. The fine-grained microstructure is the result of a suitably selected recrystallization annealing temperature (950 °C) after cold rolling. Furthermore, the fine grain microstructure can be attributed to chromium alloying, which has positive effects on grain size reduction, as demonstrated by Wang et al [22].

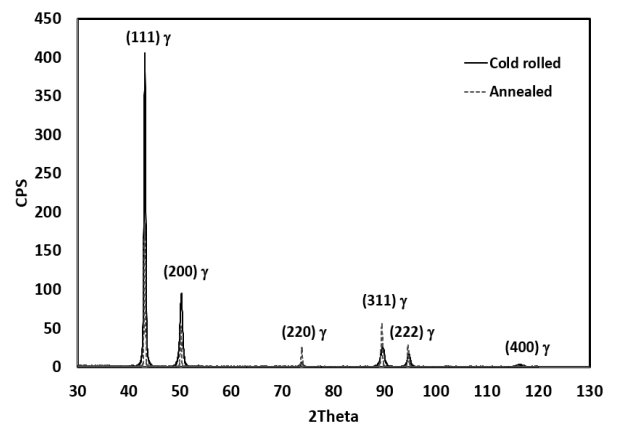


Fig. 2 X-ray diffraction patterns of annealed and cold rolled states of experimental steel

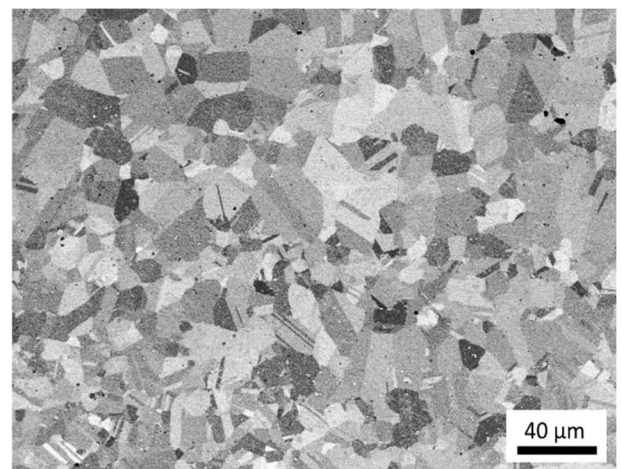


Fig. 3 Microstructure of experimental steel captured in back-scattered electrons regime

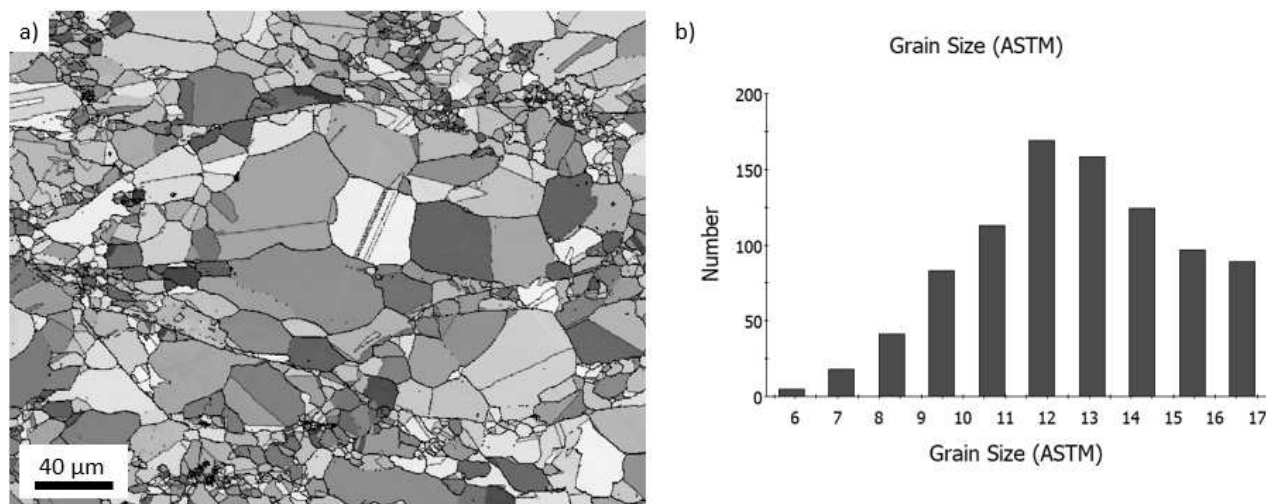


Fig. 4 Microstructure of experimental steel captured in back-scattered electrons regime

3.3 Corrosion properties

During the corrosion resistance test, the polarization resistance (R_p), cyclic polarization curve (Cp) and corrosion potential (EOC) of the supplied samples

were measured. The corrosion potential (E_{corr}), polarization resistance (R_p) and corrosion current density (i_{corr}) were calculated from the test (Table 3). The final values are the average of three measurements.

Tab. 3 Results of electrochemical measurements of experimental steel at 21 °C

Parameter	E_{corr} [mV]	R_p [$\Omega.m^2$]	i_{corr} [$\mu A.cm^{-2}$]
Value	-374.1 ± 31.6	2.97 ± 0.33	0.17 ± 0.05

During the corrosion resistance test, the polarization resistance (R_p), cyclic polarization curve (Cp) and corrosion potential of the samples were measured. The corrosion potential (E_{corr}), polarization resistance (R_p) and corrosion current density (i_{corr}) were calculated from the test (Table 3). The resulting values are the average of the three measurements.

compared to other studies [24-26]. Also the polarization resistance R_p 2.97 $\Omega.m^2$ is almost 6 times higher in comparison to the results in our previous paper [23]. A higher polarization resistance indicates greater resistance to corrosion, while a lower polarization resistance indicates increased susceptibility to corrosion. The higher corrosion resistance of this steel may be due to the higher molybdenum content, which generally has a positive effect on corrosion resistance [27]. Compared to [23], the steel in this study was also more nitrogen alloyed (0.73 here contra 0.54 wt % in [21]), which according to the study of Mujica et al. [18], Tsuchiyama et al. [16] and Yuan et al. [17] have additional effect of improving the corrosion resistance of the steel.

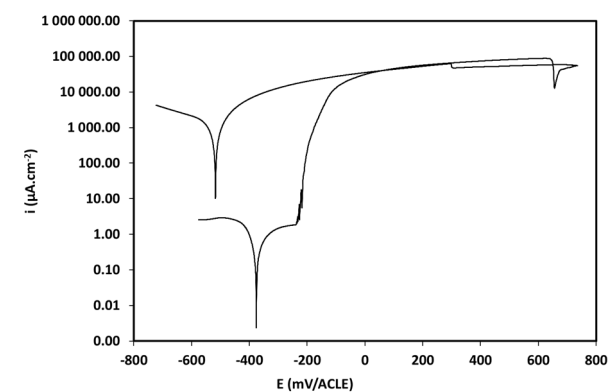


Fig. 5 Potentiodynamic polarization curves of annealed experimental steel obtained in model sea water

When comparing the measured value of corrosion current density of $0.17 \pm 0.05 \mu A.cm^{-2}$ with the authors' previous study of a steel with a slightly different chemical composition (27.5Mn, 12.9Cr, 1.1Mo, 0.54N, 0.33C), where the measured value of i_{corr} was $0.34 \mu A.cm^{-2}$ [23], the corrosion resistance of the experimental TWIP steel in this study is higher. This steel also shows better corrosion properties

4 Conclusion

In the presented research, a new steel with TWIP effect and increased corrosion resistance was developed and tested. This experimental steel is characterized in particular by the following properties:

- The steel is alloyed mainly with 27.78 wt.% manganese, 12.7 wt.% chromium, 1.26 wt. % molybdenum and 0.73 wt % nitrogen.
- Sheets produced from this experimental steel achieve an excellent combination of high strength of 941.5 MPa and ductility of 54.5 %.

The strength and yield strength parameters are equivalent to high strength dual-phase steels used for automotive body components. However, the ductility (and thus the ability to absorb impact) is more than 3 times higher compared to DP steels.

- The microstructure of the steel is fully austenitic both in the as-rolled condition and in the condition after recrystallization annealing at 950 °C without the presence of transformation-induced martensite (alpha' or epsilon). The absence of epsilon martensite gives this steel the ability to resist hydrogen attack and avoid hydrogen delayed fracture.
- The appropriate choice of the recrystallization annealing temperature (950 °C) and chromium alloying results in a very fine-grained microstructure reaching average austenitic grain size is $G = 12.6$ according to ASTM E112
- In terms of corrosion properties, this experimental TWIP steel exhibits good corrosion current density parameters of $0.17 \pm 0.05 \mu\text{A}\cdot\text{cm}^{-2}$ and polarization resistance R_p 2.97 $\Omega\cdot\text{m}^2$. The values of these parameters are significantly better compared to other corrosion resistance enhancement studies of TWIP steels and they are the result of alloying with chromium, molybdenum and nitrogen.

Acknowledgement

The paper was supported from ERDF: Research of advanced steels with unique properties, No. CZ02.1.01/0.0/0.0/16_019/0000836. This research was also funded by SLOVENIAN RESEARCH AGENCY, grant number P2-0132 and L2-4445.

References

- [1] HOFMANN, H., MATTISSEN, D., SCHAUMANN, T. W. (2006). Advanced cold rolled steels for automotive applications. In: *Materwiss. Werkstofftech.*, vol. 37, no. 9, pp. 716–723, doi: 10.1002/mawe.200600057
- [2] CORNETTE, D., CUGY, P., HILDENBRAND, A., BOUZEKRI, M., LOVATO G., (2005). Ultra High Strength FeMn TWIP Steels for automotive safety parts. In: *Rev. Métallurgie*, doi: 10.1051/metal:2005151
- [3] DE COOMAN, B. C., Estrin, Y., KIM, S. K. (2018). Twinning-induced plasticity (TWIP) steels. In: *Acta Mater.*, vol. 142, pp. 283–362, doi: 10.1016/j.actamat.2017.06.046
- [4] JOOST, W. J. (2012). Reducing Vehicle Weight and Improving U.S. Energy Efficiency Using Integrated Computational Materials Engineering. In: *Journal of Metals* vol. 64, no. 9, pp. 1032–1038, doi: 10.1007/s11837-012-0424-z
- [5] BOUAZIZ, O., Guelton, N. (2001). Modelling of TWIP effect on work-hardening. In: *Mater. Sci. Eng. A*, vol. 319–321, pp. 246–249, doi: 10.1016/S0921-5093(00)02019-0
- [6] CHUN, Y. S., KIM, J. S., PARK, K. T., LEE, Y. K., LEE, C. S. (2012). Role of ϵ martensite in tensile properties and hydrogen degradation of high-Mn steels. In: *Mater. Sci. Eng. A*, vol. 533, pp. 87–95, doi: 10.1016/j.msea.2011.11.039
- [7] ESSOUSSI, H., Ettaqi, S., ESSADIQI, E. (2018). The effect of alloying elements on the stacking fault energy of a TWIP steel, In: *Procedia Manufacturing*, vol. 22, pp. 129-134, doi: 10.1016/j.promfg.2018
- [8] YUAN, X., ZHAO, Y., LI, X., CHEN, L. (2017). Effect of Cr on mechanical properties and corrosion behaviors of Fe-Mn-C-Al-Cr-N TWIP steels. In: *J. Mater. Sci. Technol.*, vol. 33, no. 12, pp. 1555–1560, doi: 10.1016/j.jmst.2017.08.004
- [9] JUNG, Y-S., KANG, S., JEONG, K., JUNG, J-G., LEE, Y-K. (2013). The effects of N on the microstructures and tensile properties of Fe–15Mn–0.6C–2Cr–xN twinning-induced plasticity steels, In: *Acta Materialia*, vol 61, Issue 17, pp. 6541–6548, doi:10.1016/j.actamat.2013.07.036
- [10] SEUNG-JOON, L., HIDETOSHI, F., KOHSAKU, U. (2018). Thermodynamic calculation of the stacking fault energy in Fe-Cr-Mn-C-N steels. In: *Journal of Alloys and Compounds*, pp. 749-776, doi: 10.1016/j.jallcom.2018.03.296
- [11] WAN, H., Cai, Y., SONG, D., CHEN, C. (2020) Effect of Cr/Mo carbides on corrosion behaviour of Fe_Mn_C twinning induced plasticity steel, in *Corrosion Science*, vol. 167, doi:10.1016/j.corsci.2020.108518
- [12] LI, D. G., WANG, J. D., CHEN, D. R., LIANG, P. (2015). Molybdenum addition enhancing the corrosion behaviors of 316 L stainless steel in the simulated cathodic

- environment of proton exchange membrane fuel cell. In: *Int. J. Hydrogen Energy*, doi: 10.1016/j.ijhydene.2015.01.165
- [13] WANG, X., SUN, X., Song, C., CHEN, H., TONG, S., HAN, W., PAN, F. (2018) Evolution of microstructures and mechanical properties during solution treatment of a Ti–V–Mo-containing high-manganese cryogenic steel, in: *Materials Characterization*, vol. 135, pp 287-294, doi:10.1016/j.matchar.2017.11.054
- [14] YUAN, X., Zhao, Y., LI, X., CHEN, L. (2017) Effect of Cr on mechanical properties and corrosion behaviors of Fe–Mn–C–Al–Cr–N TWIP steels, in: *Journal of Materials Science & Technology*, vol. 33, Issue 12, pp 1555-1560, doi: 10.1016/j.jmst.2017.08.004
- [15] TSAY, G., LIN, C., Chao, C., LIU, T., (2010). A new austenitic FeMnAlCrC alloy with high-strength, high-ductility, and moderate corrosion resistance, in: *Materials Transactions*, doi: 10.2320/matertrans.M2010199.
- [16] TSUCHIYAMA, T., ITO, H., KATAOKA, K., TAKAKI, S. (2003) Fabrication of Ultrahigh Nitrogen Austenitic Steels by Nitrogen Gas Absorption into Solid Solution, in: *Metallurgical and Materials Transactions A*, vol 34A, pp 2591 - 2599
- [17] YUAN, X., CHEN, L., Zhao, Y., DI, H., ZHU, F. (2015) Influence of annealing temperature on mechanical properties and microstructures of a high manganese austenitic steel, in: *Journal of Materials Processing Technology*, vol. 217, pp 278-285
- [18] MUJICA, L. WEBER, S., HUNOLD, G. THEISEN, W. (2011) Development and characterization of novel corrosion-resistant TWIP steels, in: *Steel Research International*, doi:10.1002/srin.201000219
- [19] ÖZTÜRK, E., ARIKAN, H. (2023) Investigation of mechanical properties of laser welded dual-phase steels at macro and micro levels, *Optics & Laser Technology*, vol. 157, 108713, doi:10.1016/j.optlastec.2022.108713
- [20] KUČEROVÁ, L., TICHÁ, I., STEHLÍK, A. (2021) Effect of Various Heat and Thermo-mechanical Treatments on Low Alloyed CMnAlNb High Strength Steel, in: *Manufacturing Technology*, Vol. 21, No. 6, pp. 824-828, doi: 10.21062/mft.2021.094
- [21] KOREČEK, D., SOLFRONK, P., SOBOTKA, J. (2022) Analysis of the Dual-phase Steel DP500 Stress-strain Characteristics During the Plane Shear Test, in: *Manufacturing Technology*, Vol. 22, No. 1, doi:10.21062/mft.2022.015
- [22] WANG, X.J., Sun, X.J., SONG, C., CHEN, H., HAN, W., PAN, F. (2017) Enhancement of yield strength by chromium/nitrogen alloying in high-manganese cryogenic steel, in. *Materials Science and Engineering: A*, vil. 698, pp 110-116, doi:10.1016/j.msea.2017.05.023
- [23] PODANY, P., GREGOR, T., STUDECKY, T., DONIK, C. (2022). High Manganese TWIP Steel with Increased Corrosion Resistance. In: *Metals (Basel)*, vol. 12, no. 10, p. 1765, doi: 10.3390/met12101765
- [24] KANNAN, M. B., Raman, R. K. S., KHODDAM, S., LIYANAARACHCHI, S. (2013). Corrosion behavior of twinning-induced plasticity (TWIP) steel. In: *Mater. Corros.*, vol. 64, no. 3, pp. 231–235, doi: 10.1002/maco.201106356
- [25] BOSCH, J., MARTIN, U., APERADOR, W., BASTIDAS, J. M., RESS, J., BASTIDAS, D. M. (2021). Corrosion behavior of high-Mn austenitic Fe–Mn–Al–Cr–C steels in NaCl and NaOH solutions. In: *Materials (Basel)*, doi: 10.3390/ma14020425
- [26] FAJARDO, S., Llorente, I., JIMÉNEZ, J. A., CALDERÓN, N., HERRÁN-MEDINA, D., BASTIDAS, J. S., RESS, J. (2020). Influence of chromium on the passivity of thermo-mechanically processed high-Mn TWIP steels, In: *Appl. Surf. Sci.*, doi: 10.1016/j.apsusc.2020.145852
- [27] LI, D. G., WANG, J. D., Chen, D. R., LIANG, P. (2015). Molybdenum addition enhancing the corrosion behaviors of 316 L stainless steel in the simulated cathodic environment of proton exchange membrane fuel cell. In: *Int. J. Hydrogen Energy*, doi: 10.1016/j.ijhydene.2015.01.165